

NEAR-INFRARED POLARIMETRY OF STAR FORMATION REGIONS

Cecilia Colomé and Paul M. Harvey

Department of Astronomy, University of Texas at Austin

RESUMEN

Hemos adaptado un polarímetro lineal a la nueva cámara infrarroja (IRC2) de la Universidad de Tejas. Uno de los proyectos actuales con este nuevo instrumento es el obtener mapas de polarización en el cercano infrarrojo de alta resolución angular en determinadas regiones galácticas de formación estelar reciente (L1551/IRS 5, NGC 2023, NGC 2024 y LkH α 101). Las primeras observaciones polarimétricas fueron realizadas en noviembre de 1992, usando el telescopio de 2.7 metros del Observatorio McDonald, y la reducción de datos aun no concluye. A continuación presentamos una breve descripción de las características de la nueva cámara, así como el procedimiento en la reducción de los datos y los resultados preliminares de la polarimetría de L1551/IRS 5.

ABSTRACT

We have adapted a linear polarimeter to the new infrared camera (IRC2) of the University of Texas at Austin. One of the current projects using this new instrument is to obtain high angular resolution polarization maps of selected galactic star formation regions (L1551/IRS 5, NGC 2023, NGC 2024 and LkH α 101). The first polarimetric measurements were obtained in November of 1992 at the 2.7 m telescope of McDonald Observatory, and the data reduction is still in progress. This paper provides a brief overview of both the polarimetric near-infrared camera and the data reduction procedure, and also some preliminary results on the polarimetric imaging of L1551/IRS 5.

Key words: **INFRARED: INTERSTELLAR: CONTINUUM — INSTRUMENTATION: POLARIMETERS — STARS: FORMATION**

1. INTRODUCTION

As an application of the new near-infrared (NIR) polarimetric camera we have begun a study of galactic star forming regions. The first set of these objects includes L1551/IRS 5, NGC 2023, NGC 2024 and LkH α 101. These objects are known to exhibit large polarization ($P \geq 15\%$), indicating that the polarization is mainly caused by scattering of light by dust grains. By assuming a reasonable geometry and dust grains properties, one can derive the column density of the scattering dust from the measurement of the polarization as a function of distance from the central luminosity source. The main goal of our study is to determine density gradients in the immediate environment of these objects. These density gradients can be directly compared with those predicted by star formation models. We will use the interstellar and circumstellar dust as a probe in infrared sources. Our approach is to combine the far-infrared high angular resolution techniques, developed by the infrared group at the University of Texas at Austin on the NASA Kuiper Airborne Observatory, with the new polarimetric NIR imaging camera.

2. INSTRUMENTATION

2.1. The Camera

The new NIR imaging camera of the University of Texas at Austin employs a 256×256 HgCdTe detector array (NICMOS 3). This camera is operated at the Cassegrain focus of the 2.7 m telescope at McDonald Observatory, providing an image scale of $0.4''$ pixel $^{-1}$ and a $\sim 100'' \times 100''$ field of view.

Given the low readout noise and dark current, the sensitivity of IRC2 is mainly background limited. Assuming that all the light of a source falls into one pixel and a signal-to-noise ratio of 1 in 0.5 sec of integration time, the corresponding magnitudes at J, H and K are: $m_J \sim 19.7$, $m_H \sim 18.8$ and $m_K \sim 17.6$. The available IRC2 broad band filters are the standard J ($\delta\lambda=0.3\mu\text{m}$), H ($\delta\lambda=0.3\mu\text{m}$) and K ($\delta\lambda=0.4\mu\text{m}$). There are two extra K filters with a slightly narrower bandwidth, commonly named as: Short-K ($\lambda: 2.00\text{--}2.32\mu\text{m}$) and Continuum-K ($\lambda: 2.23\text{--}2.29\mu\text{m}$). In addition, there are 5 narrow band filters (all of them with 1% bandwidth) H_2 , $v=1\text{--}0$ S(1) @ $2.122\mu\text{m}$, H_2 , $v=2\text{--}1$ S(1) @ $2.248\mu\text{m}$, [FeII] @ $1.644\mu\text{m}$, CO (2-0) bandhead @ $2.295\mu\text{m}$ and Br γ @ $2.165\mu\text{m}$.

2.2. The Polarimeter

The polarimeter adapted to IRC2 is a cold (@ 70 K) wire grid, placed inside the camera dewar. The analyzer is an ambient temperature rotatable half-wave plate. This component is placed between the telescope and the entrance window of the camera, in this way minimizing any instrumental polarization. The substrate material of the wire grid is calcium fluoride with an 85% transmission efficiency. It provides a degree of polarization of 93% at $1.5\mu\text{m}$ and slightly higher at longer wavelengths. The analyzer is an achromatic half-wave plate made from magnesium fluoride and crystal quartz. The total retardation (theoretical and due to manufacturing errors) is from 0.617 to 0.419 waves over the $1.0\text{--}2.5\mu\text{m}$ range.

3. DATA ACQUISITION AND REDUCTION

Polarimetric images of L1551/IRS 5, NGC 2023, NGC 2024 and LkH α 101 were taken during five nights in November of 1992. The BN-KL object and OH 0739-14 were observed for the position angle calibration. A set of infrared standard stars was also observed each night for flux calibration and for estimates of the instrumental polarization.

Each object was observed through three broad-band filters: J, H, and K. The procedure was to take a set of short exposures (≤ 4 seconds) at 9 separate positions of the half-wave plate with the respect to the wire grid. Each position interval corresponds to a rotation of 22.5° of the half-wave plate, which translates into a 45° rotation of the plane of polarization as seen from the wire grid. This implies that each suite of images provides two independent data sets cycling completely through four independent polarizer position angles. Nodding between object and sky positions was employed for each polarizer position angle. Several dark frames of the same integration time were taken before and after observing each object. Flat-fields at each wavelength were constructed by subtracting the dark from the sky frames and normalizing by their median value. For each individual image bad pixels were corrected by an interpolation routine using the values of the healthy neighbouring pixels. After sky-subtraction and flat-fielding, the images of each set of the same position angle were then cross-correlated. This procedure allowed us to minimize the image blur due to the seeing ($\leq 1''$). An average of all the resulting images of the same position angle was constructed. If we denote as P_1 , P_2 , P_3 and P_4 the four polarized images which differ by steps of 45° in position angle, with the intensity in these images at pixel x,y being P_k , for $k=1\text{--}4$, we can calculate the polarization at each pixel using the formulae:

$$I = P_2(x,y) + P_4(x,y) = P_1(x,y) + P_3(x,y)$$

$$Q = P_1(x,y) - P_3(x,y), U = P_2(x,y) - P_4(x,y)$$

$$\tan 2\theta_0 = U/Q, P = (Q^2 + U^2)^{1/2}/I$$

where I , Q and U are the stokes parameters, θ_0 is the polarization position angle, and P is the percent polarization.

4. L1551/IRS 5

This object is located in a nearby cloud ($d=140$ pc) in Taurus. It is believed to be a low mass, $\leq 2.5M_{\odot}$, pre-main-sequence star (Strom, Strom & Vrba 1976; Emerson et al. 1984). A highly collimated CO bipolar outflow was first discovered by Snell, Loren & Plambeck (1980). The orientation of the outflow is in the NE-SW direction (Snell & Schloerb 1985; Moriarty-Schieven et al. 1987). A flattened structure has been traced in emission of CS (Kaifu et al. 1984; Batrla & Menten 1985; Moriarty-Schieven et al. 1987). An ionized jet has been detected in $H\alpha$ along the direction of the south-western part of the outflow (Mundt & Fried 1983), as well as an extended nebulosity. Large polarization values have been detected at optical and NIR wavelengths in L1551/IRS 5 (Nagata, Sato & Kobayashi 1983; Hodapp 1984; Campbell et al. 1988). This high degree of polarization can only be explained by scattering of light by dust grains. Our goal in this object was to obtain new high angular resolution NIR polarimetric data over a wider spatial scale that had been previously achieved, hoping to trace the polarization over the nebulosity associated with IRS 5. The NIR polarization of the nebulosity, if existent, was below our detection limit. We could only get reliable polarimetry in the compact (but resolved) infrared source. Our polarization results agree, within the errors, with previous measurements. We did several averages of the polarization at each wavelength, varying the effective "aperture" in the measurements. The polarization remains constant from a $1''$ (seeing limitation) diameter up to $10''$ (maximum value for which the polarization maps have useful signal-to-noise ratio). This is true for at least the J and H bands. More statistical analysis is required for the K band data. This confirms the belief that there is no significant contribution to the emission from a central, unpolarized source directly rather than via scattering. Table 2 summarizes our results together with the available polarimetry of L1551/IRS 5.

5. SUMMARY

The preliminary results from our high spatial imaging of L1551/IRS 5 confirm previous observations which show that IRS 5 is spatially resolved and elongated (Moneti et al. 1988). The direction of the elongation is $\sim 135^{\circ}$. Our results from the NIR polarimetry of L1551/IRS 5 indicate that practically all the polarization is due to scattering and confirm previous observational results (Hodapp 1984) namely that the NIR polarization does not depend on aperture. Our measurements of the NIR polarization angle ($150^{\circ} - 160^{\circ}$) also agrees with previous measurements. As it has been pointed out before by several authors, this position angle is approximately perpendicular to the direction of the CO outflow in L1551/IRS 5.

6. FIGURES

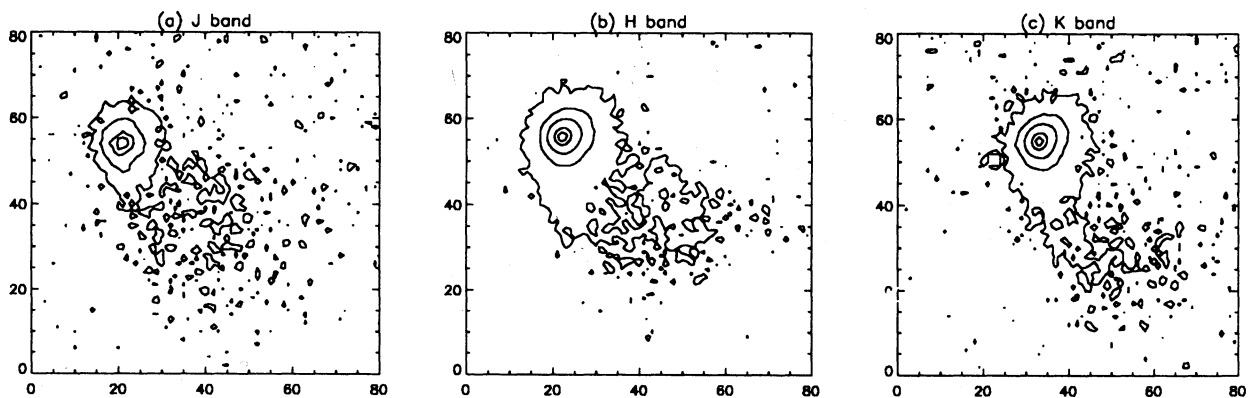


Figure 1.— Top and left of figure represent the NORTH and EAST directions respectively. Axis labels indicate pixel number. (a) L1551/IRS 5 at the J band, the isocontours represent 8, 30, 70, and 90 percent of the peak intensity. (b) and (c) L1551/IRS 5 at the H and K bands respectively, the isocontours are 1.5, 10, 30, 70, and 90 percent of peak intensity.

7. TABLES

Table 1. IRC2

Pixel size: $40\mu\text{m} \times 40\mu\text{m}$
Gain: ~ 6 electrons per data bit
Photon detection range: $1 - 2.5\mu\text{m}$
Quantum efficiency: $\sim 50\%$ @ K, slightly lower @ J and H.
Readout noise: ~ 30 electrons
Dark current: $2-5$ electrons sec^{-1} pixel $^{-1}$
Minimum integration time (imaging mode): 0.34 sec

Table 2. Available Polarimetry of L1551/IRS5

Band	P(%)	P.A.	Aperture	Reference
I	12 ± 3	$147^\circ \pm 5^\circ$	8"	1
"	7	137°	4"	1
J	26 ± 2	150°	5"	this work
H	28 ± 1	155°	5"	this work
"	28 ± 2	159°	8"	2
"	20 ± 2	$156^\circ \pm 3^\circ$	3".9	3
"	22 ± 2	157°	5".6	3
"	20 ± 2	155°	11".6	3
K	24 ± 0.7	161°	8"	2
"	21 ± 2	$158^\circ \pm 3$	11".6	3
"	23 ± 1	156°	5"	this work
L'	19 ± 2	167°	8"	2

References: 1) Campbell et al. (1988); 2) Nagata, Sato and Kobayashi (1983); 3) Hodapp (1984).

REFERENCES

- Batrla W., & Menten, K.M. 1985, ApJ, 298, L5
 Campbell, B., Persson, S.E., Strom, S.E., & Grasdalen, G. 1988, AJ, 95, 1173
 Emerson, J.P., et al. 1984, ApJ, 278, L49
 Kaifu, N., et al. 1984, A&A, 134, 7
 Nagata T., Sato S., & Kobayashi Y. 1983, A&A, 119, L1
 Moriarty-Schieven, G.H., Snell, R.L., Strom, S.E., & Grasdalen, G.L. 1987, ApJ, 317, L95
 Mundt, R., & Fried, J.W. 1983, A&A, 81, 320
 Strom, K.M., Strom, S.L., & Vrba, F.J. 1976, A&A, 81, 320
 Snell, R.L., Loren, R.B., & Plambeck, R.L. 1980, ApJ, 288, L51
 Moneti, A., Forrest, W.J., Pipher, J.L., & Woodward, C.E. 1988, ApJ, 327, 870

Cecilia Colomé and Paul M. Harvey: University of Texas at Austin, Astronomy Dept., Austin, TX 78712-1083, U.S.A.